Supplement of Geosci. Model Dev. Discuss., 8, 3147–3196, 2015
http://www.geosci-model-dev-discuss.net/8/3147/2015/
doi:10.5194/gmdd-8-3147-2015-supplement

Geoscientific Model Development Discussions
Open Access

Supplement of

The Yale Interactive terrestrial Biosphere model: description, evaluation and implementation into NASA GISS ModelE2

X. Yue and N. Unger

Correspondence to: X. Yue (xuyueseas@gmail.com)

Supporting information

Spin-up process for YIBs-offline

We use the off-line YIBs model to obtain the initial conditions for tree height and soil pools. Vegetation carbon reaches equilibrium in a timescale of 10s years. In the model, we set a uniform initial height H_0 for each PFT (Table 1). We then run the model for 60 years with fixed CO_2 concentrations and meteorological forcing at the year 1980. By the end of the spin-up run, the year-to-year variations of global average tree height, LAI, GPP, and NPP are all within ±0.05%. Soil carbon pools evolve much more slowly and reach equilibrium on timescales of 100s years (Clark et al., 2011). In the model, we use the global soil carbon content at the top 30 centimeters developed by Batjes (2009) as the initial condition. Studies investigating terrestrial carbon fluxes usually initialize models from the preindustrial period when human perturbations are negligible and soil carbon pools are considered to be at an equilibrium state (Huntzinger et al., 2013; Sitch et al., 2015). We do not initialize our model in the same way due to the availability of hourly meteorological forcing, which starts only from 1980. In a sensitivity test, Wutzler and Reichstein (2007) applied a transient correction to the soil carbon pool so that the simulated stocks match observations. We followed a similar strategy by spinning up the model with fixed CO_2 and meteorology at the year 1980 for ~80 years until the transient NEE is equal to -2 Pg C a^{-1}, a value supported by observations and multi-model ensembles (Piao et al., 2013). The simulated carbon pools are then used as initial conditions for off-line simulations for the 1980-2011 period.

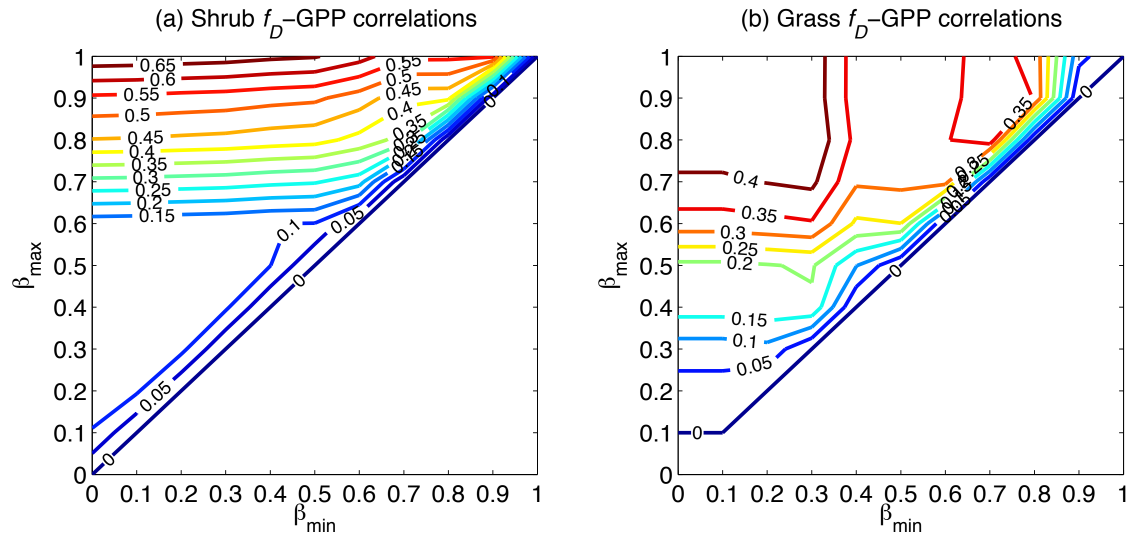

Figure S1. Average correlation coefficients between monthly GPP and drought-dependent phenology f_D at (a) shrub and (b) grass sites derived with different water stress thresholds (β_{min} and β_{max}). The results are based on 14 warm sites, 8 for shrub and 6 for grass, with annual soil temperature > 12 °C as shown in Fig. 2.

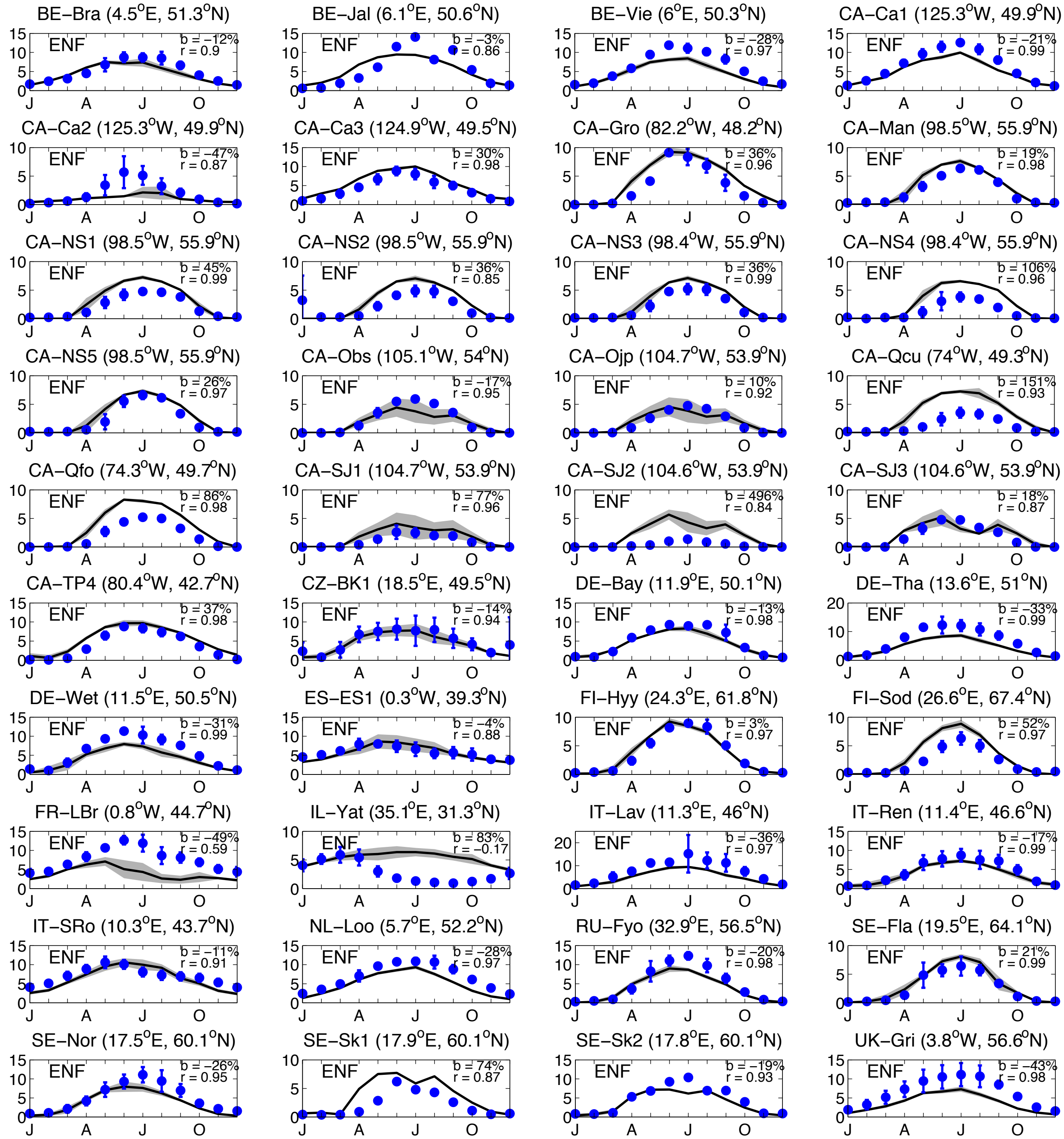

Figure S2. Comparison of simulated (solid lines) and observed (blue points) monthly gross primary productivity (GPP) at 145 sites from FLUXNET and NACP network. Both simulations and observations are averaged over the period when measurements are available (Table S1). Error bars represent one standard deviation of observations while shadings represent that of simulations. The relative bias and correlation coefficient are shown on each panel. The land types include evergreen needleleaf forest (ENF), evergreen broadleaf forest (EBF), deciduous broadleaf forest (DBF), shrublands (SHR), grasslands (GRA), and croplands (CRO). Units of GPP: g C m^{-2} day^{-1}.

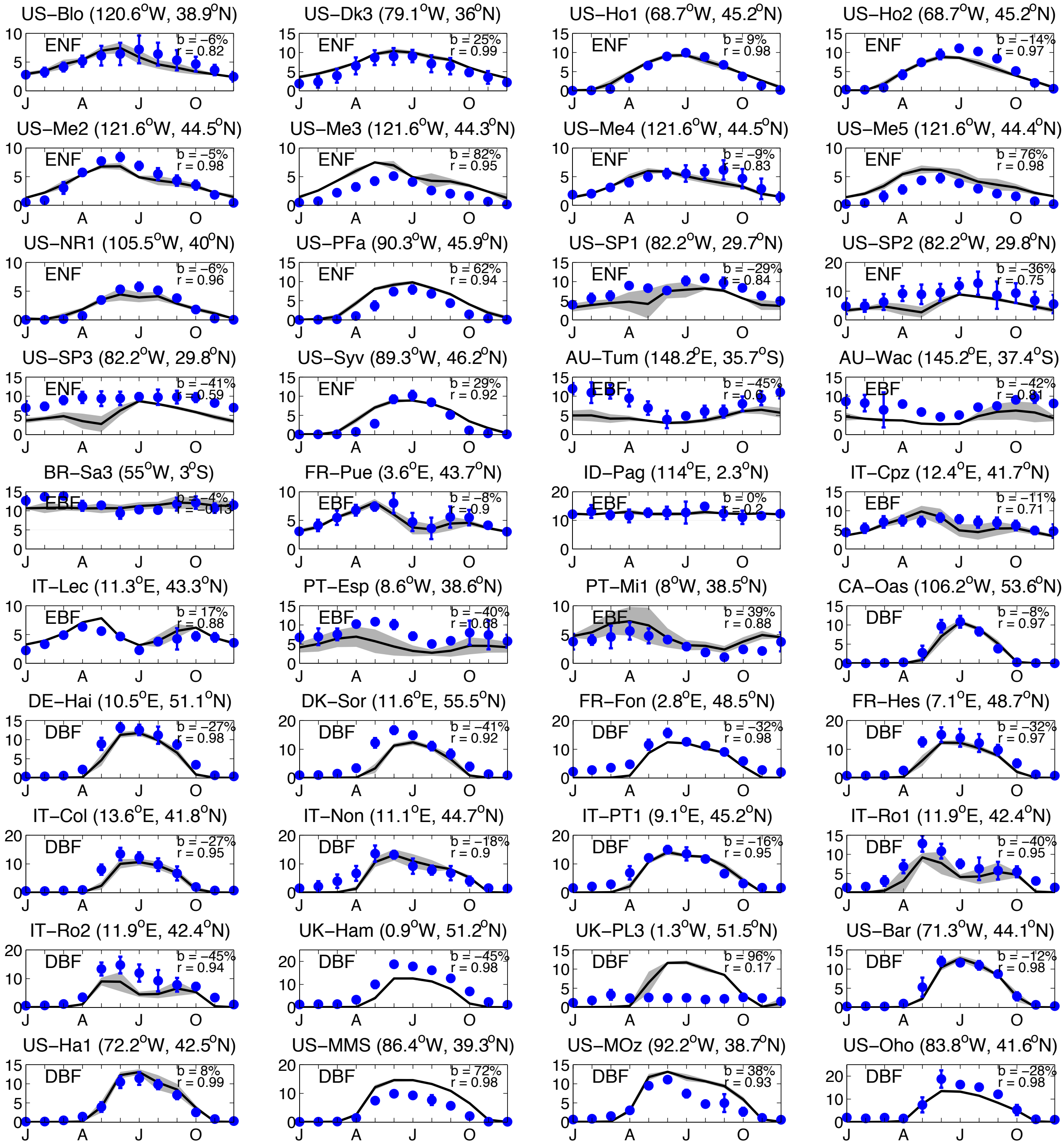

Figure S2. Continued.

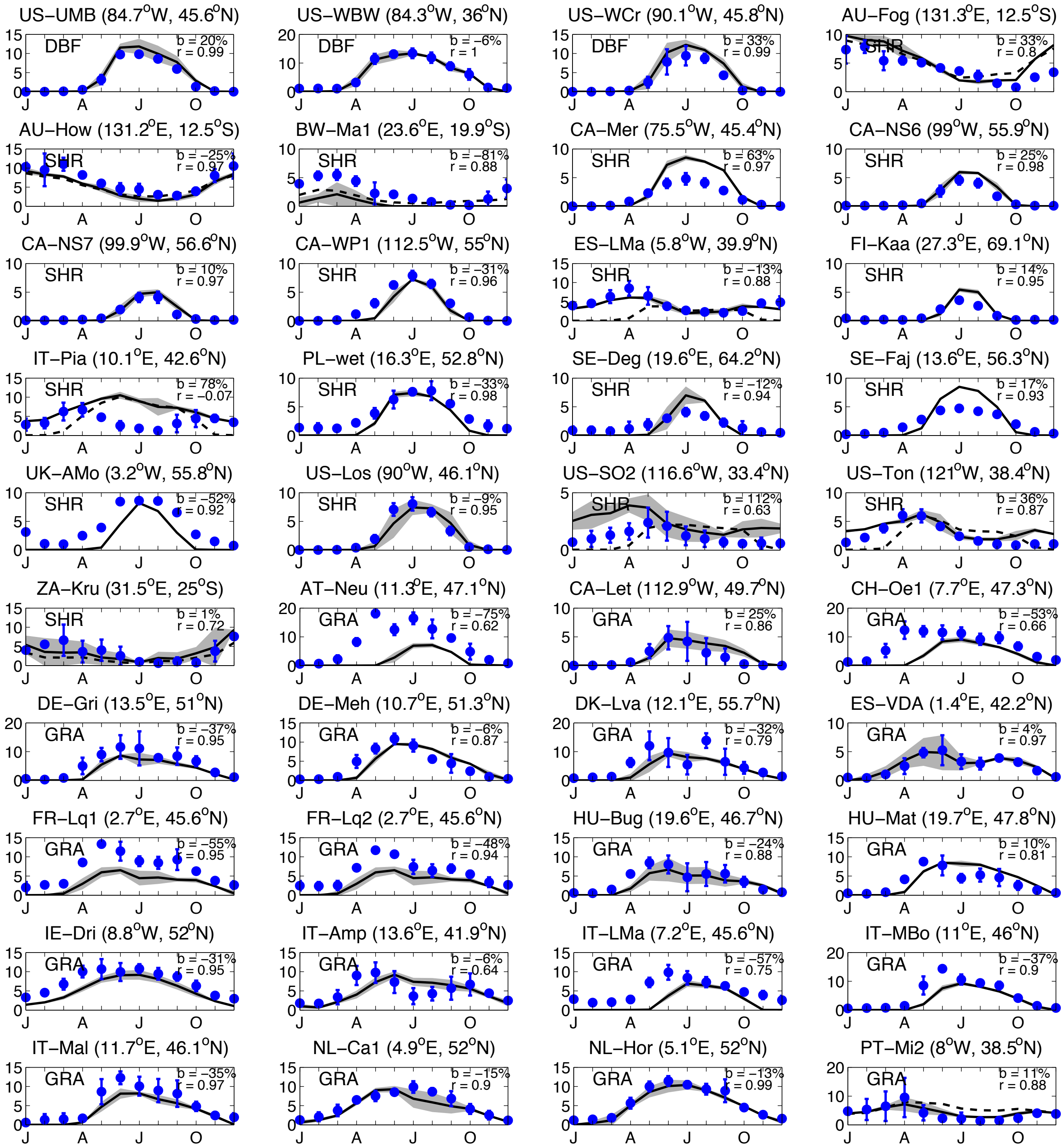

Figure S2. Continued. Dashed lines in some shrub and grass sites represent simulations with cold phenology alone.

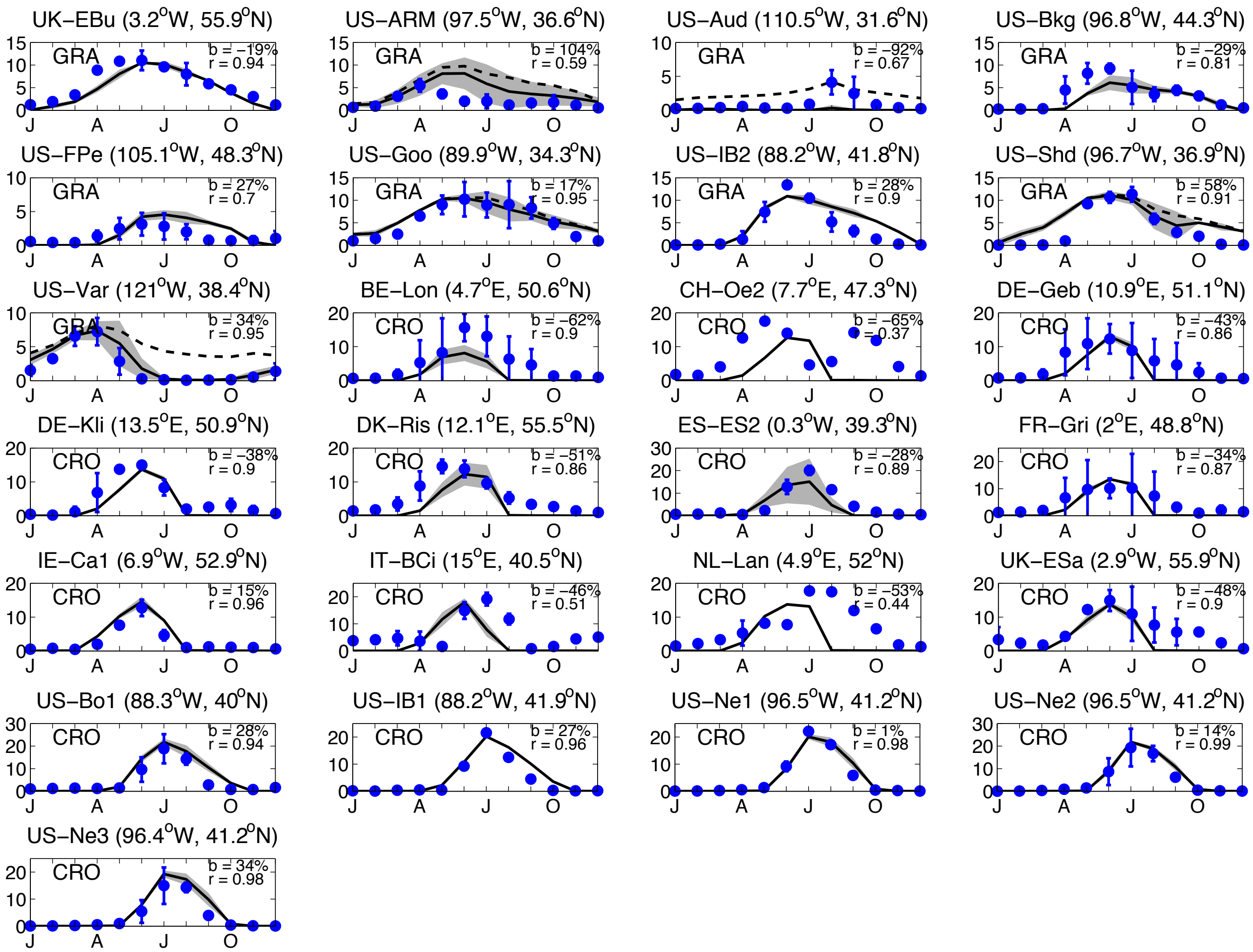

Figure S2. Continued. Dashed lines in some grass sites represent simulations with cold phenology alone.

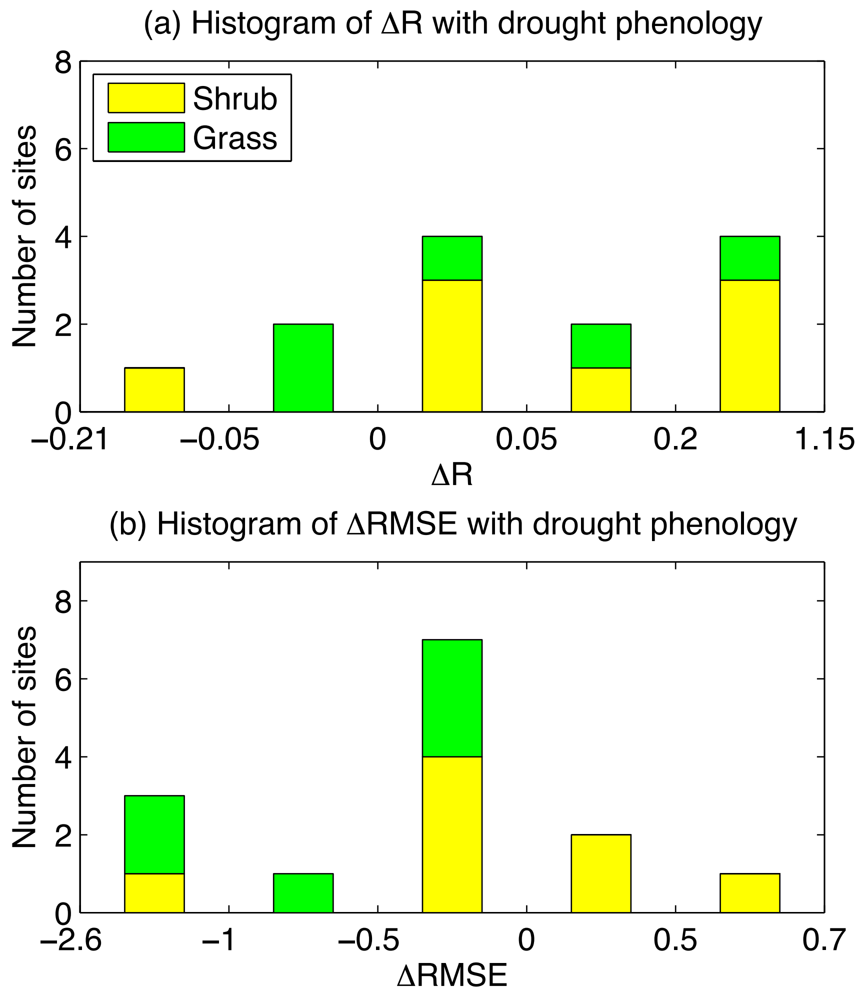

Figure S3. Histogram of changes in (a) correlation coefficients (R) and (b) root mean square error (RMSE) between the observed and simulated GPP after the inclusion of drought phenology at 14 warm sites (annual soil temperature > 12 °C). Each bar represents the number of sites where ΔR or ΔRMSE of simulations fall between the specific ranges as defined by the x-axis intervals. The minimum and maximum of ΔR or ΔRMSE are indicated as the two ends of x-axis in the plots. The distribution of x-axis is asymmetric. Detailed comparisons at these sites are presented in Fig. S2. Units of RMSE: g C m^{-2} day^{-1}.

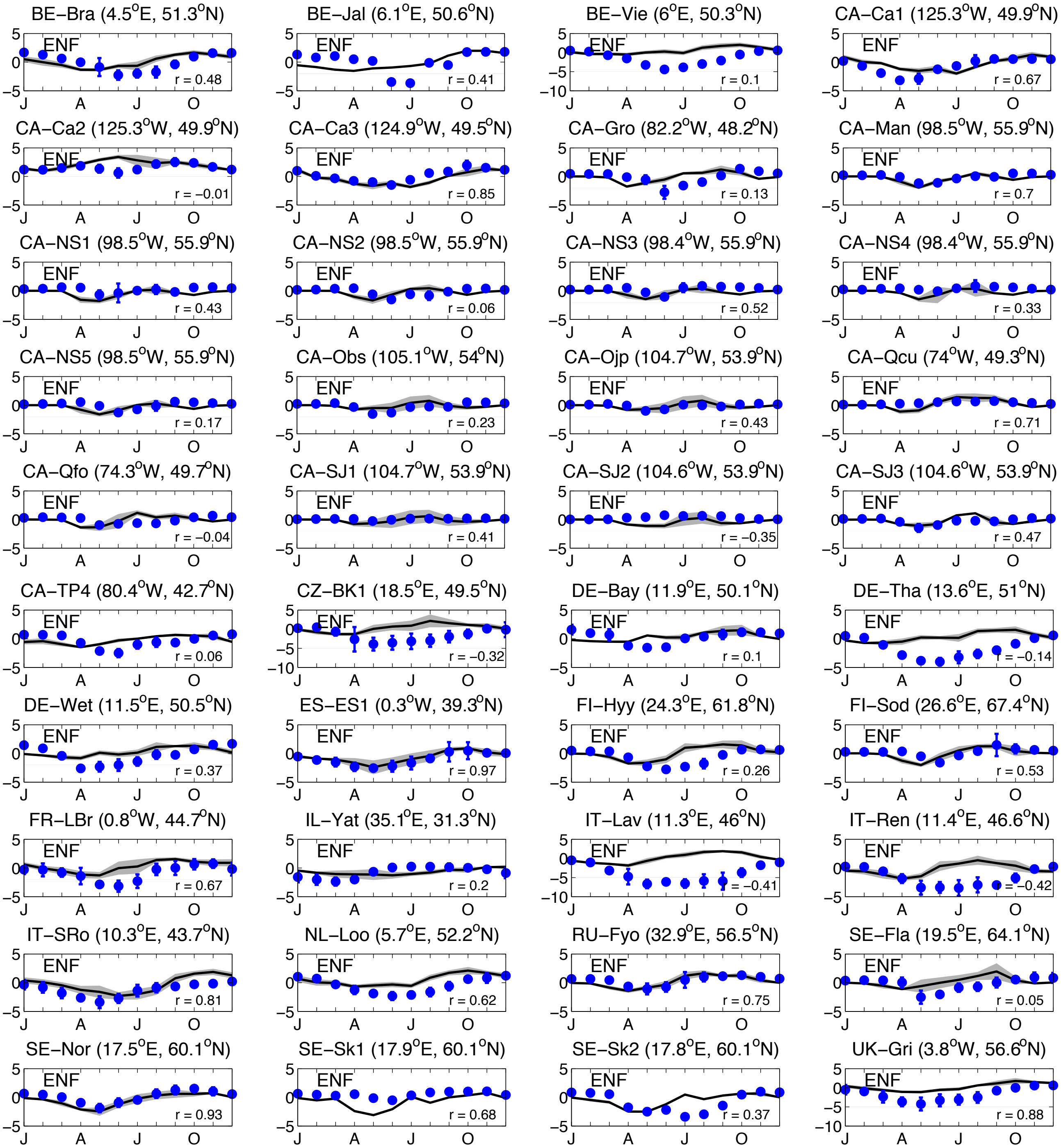

Figure S4. Comparison of simulated (solid lines) and observed (blue points) monthly net ecosystem exchange (NEE) at 145 sites from FLUXNET and NACP network. Both simulations and observations are averaged over the period when measurements are available (Table S1). Error bars represent one standard deviation of observations while shadings represent that of simulations. The relative bias and correlation coefficient are shown on each panel. The land types include evergreen needleleaf forest (ENF), evergreen broadleaf forest (EBF), deciduous broadleaf forest (DBF), shrublands (SHR), grasslands (GRA), and croplands (CRO). Units of NEE: g C m^{-2} day^{-1}.

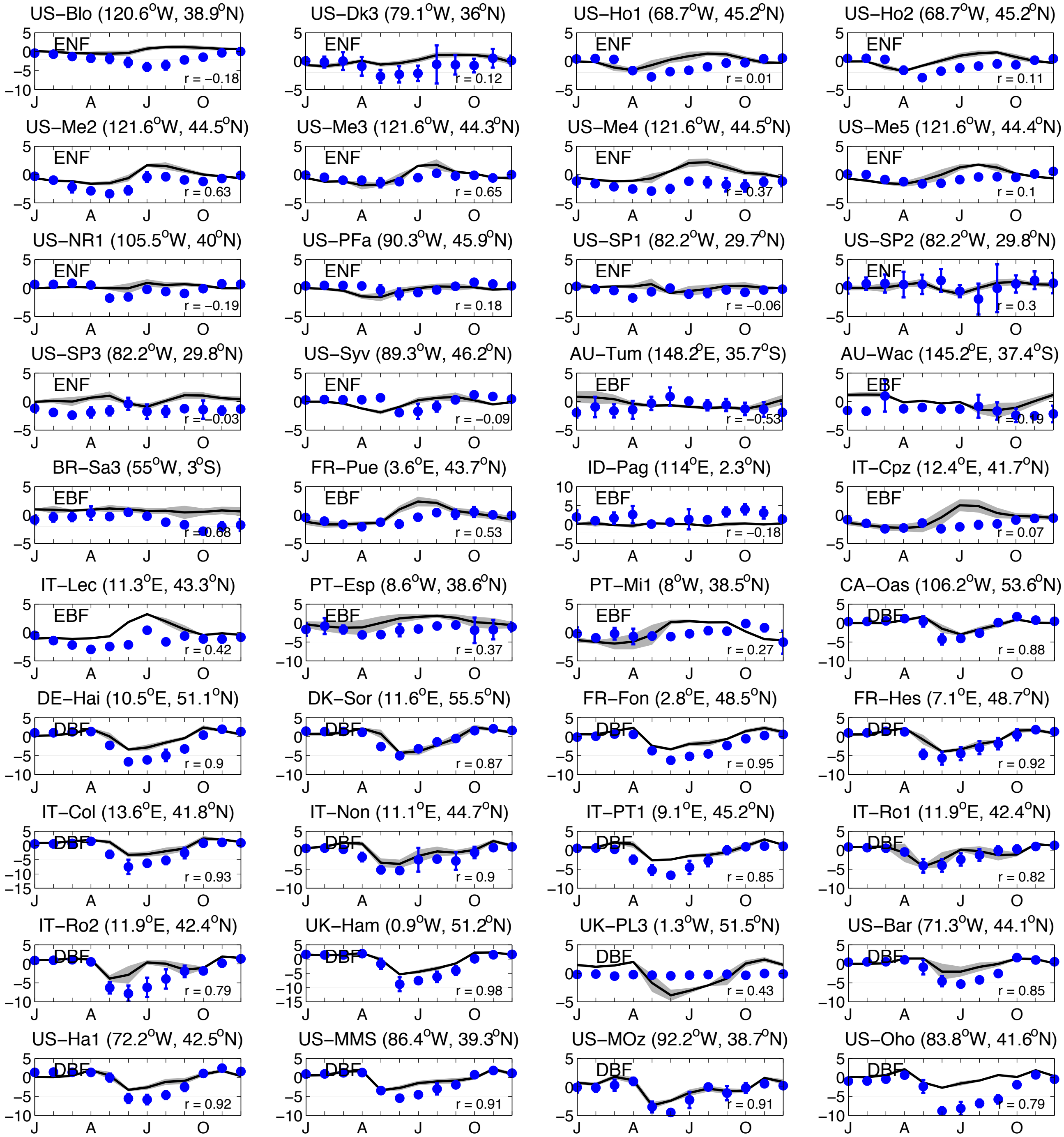

Figure S4. Continued.

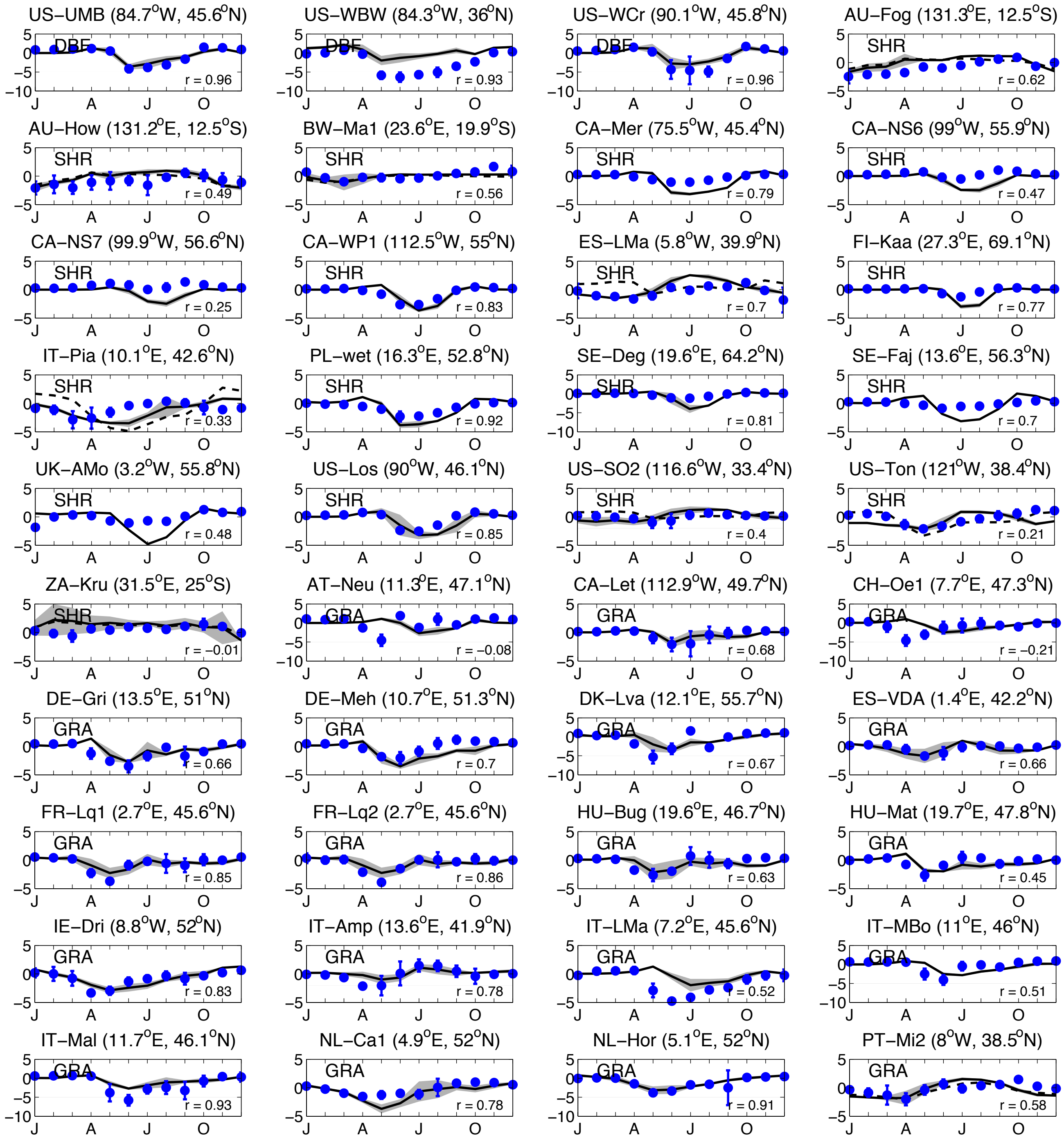

Figure S4. Continued. Dashed lines in some shrub and grass sites represent simulations with cold phenology alone.

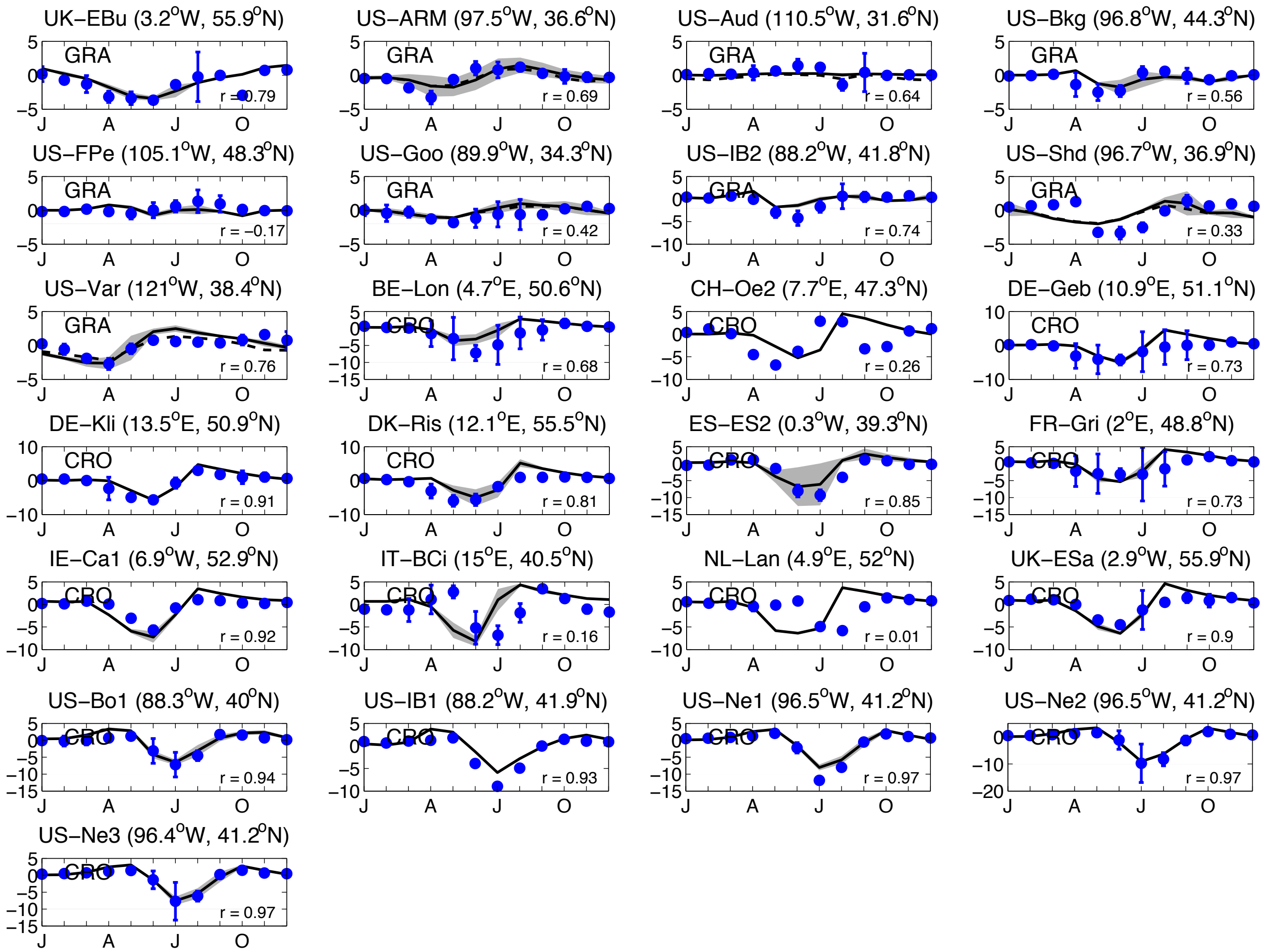

Figure S4. Continued. Dashed lines in some grass sites represent simulations with cold phenology alone.

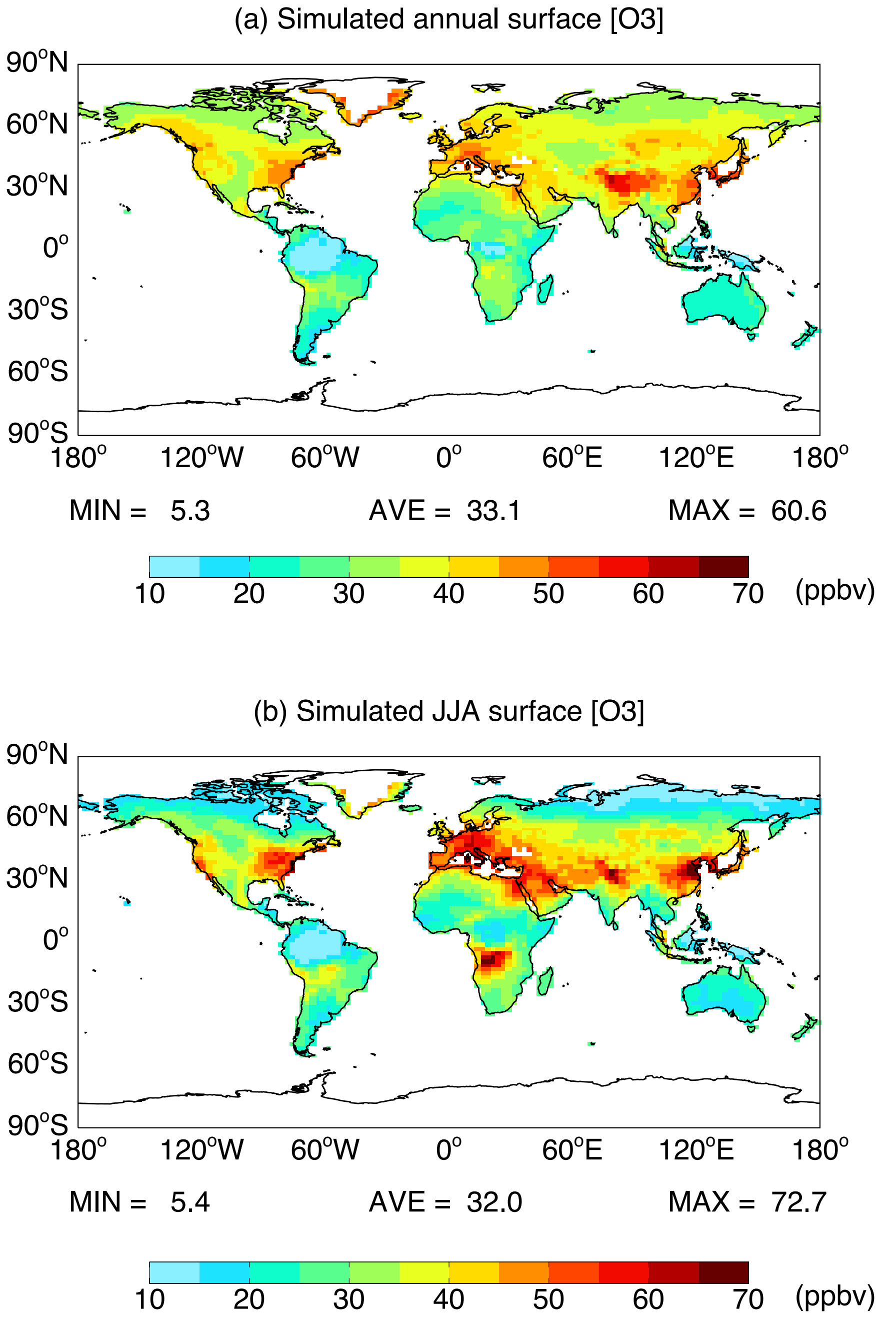

Figure S5. Simulated (a) annual and (b) June-August mean surface ozone concentrations with ModelE2.

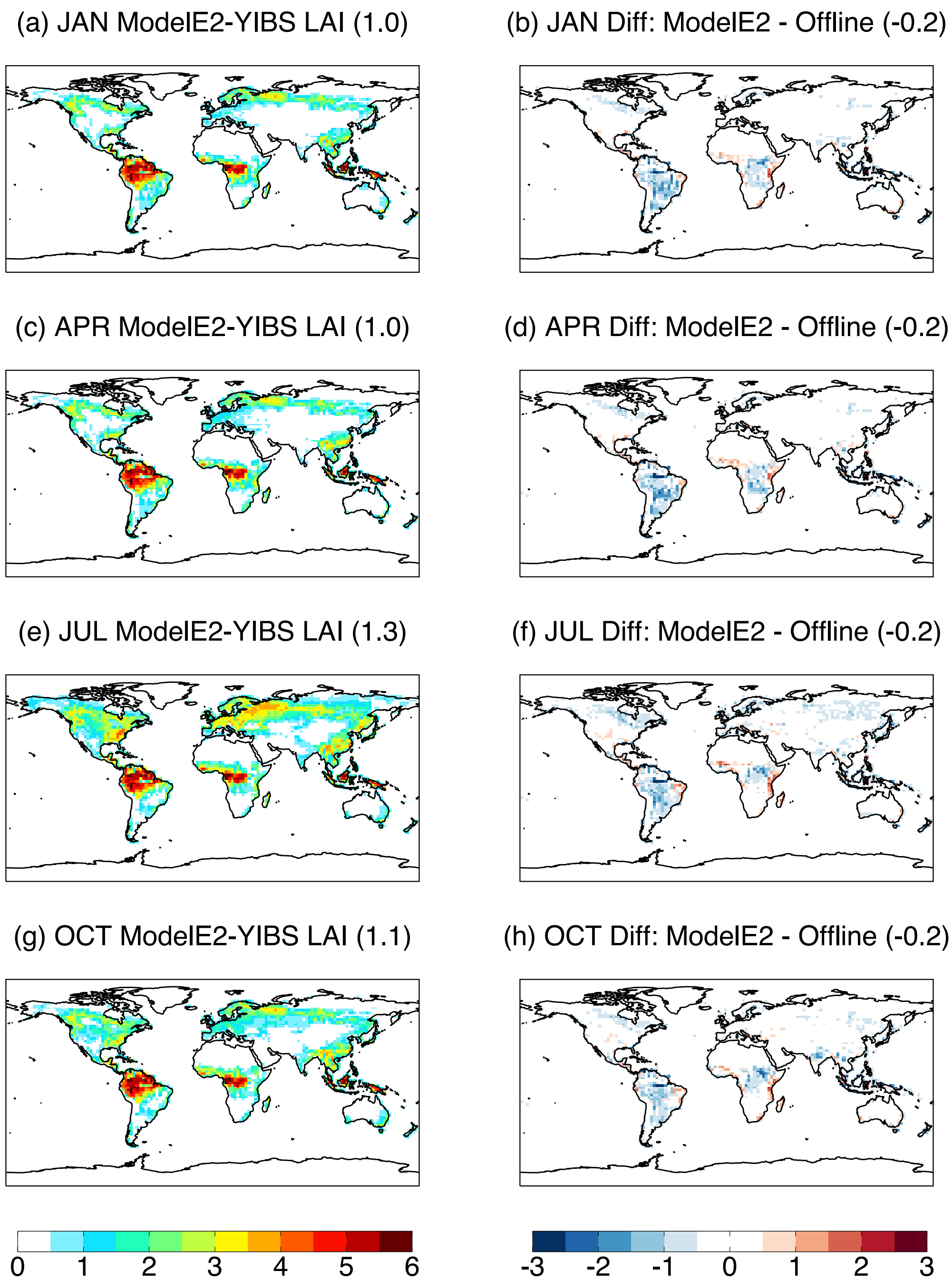

Figure S6. Simulated (left) leaf area index (LAI) with ModelE2-YIBs and (right) its differences relative to simulations with offline YIBs driven by WFDEI reanalysis for period 1996-2005. Each row represents results averaged for a specific month. Units: m^2 m^{-2}.

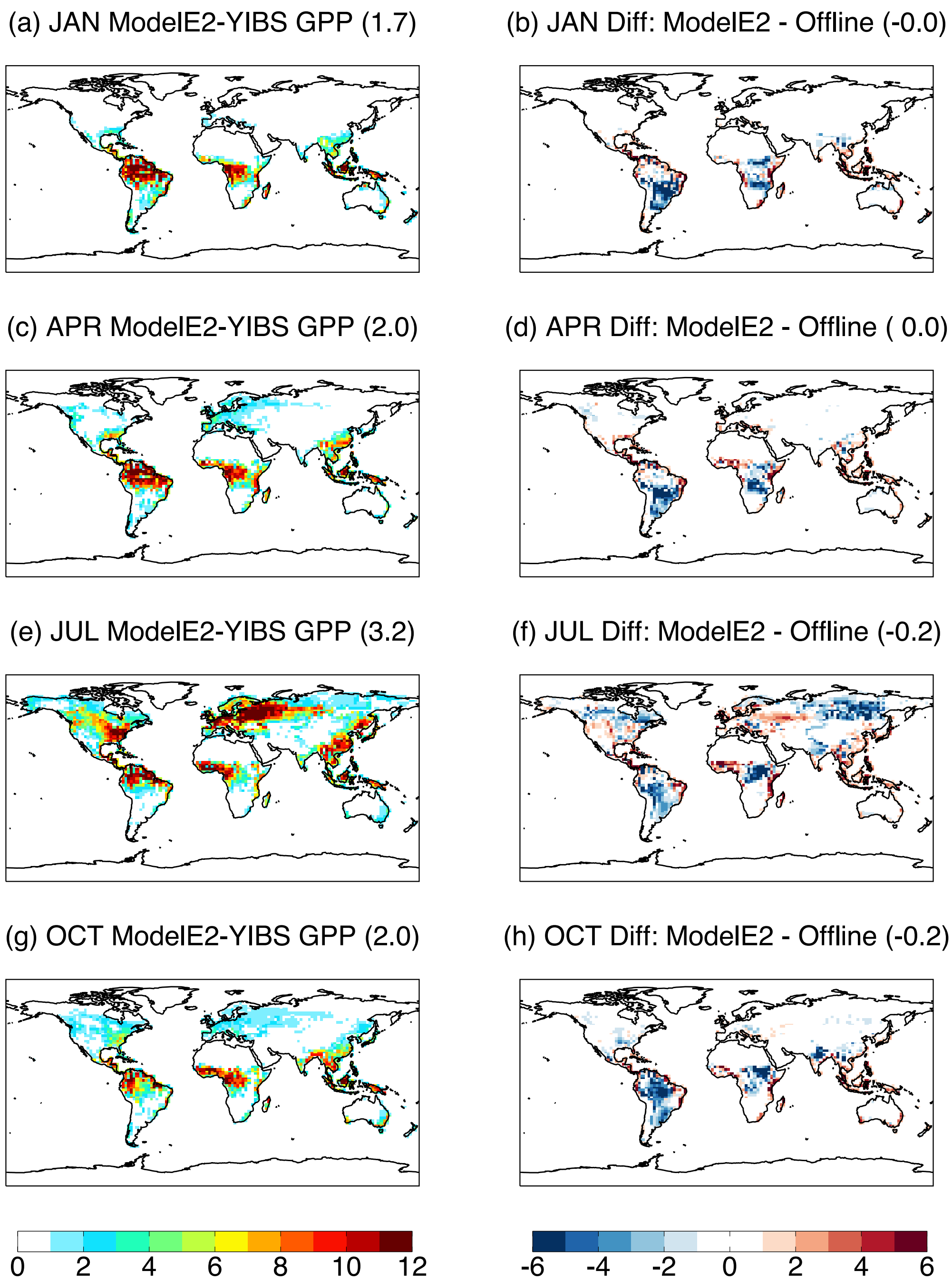

Figure S7. Simulated (left) GPP with ModelE2-YIBs and (right) its differences relative to simulations with offline YIBs driven by WFDEI reanalysis for period 1996-2005. Each row represents results averaged for a specific month. Units: g m^{-2} day^{-1}.

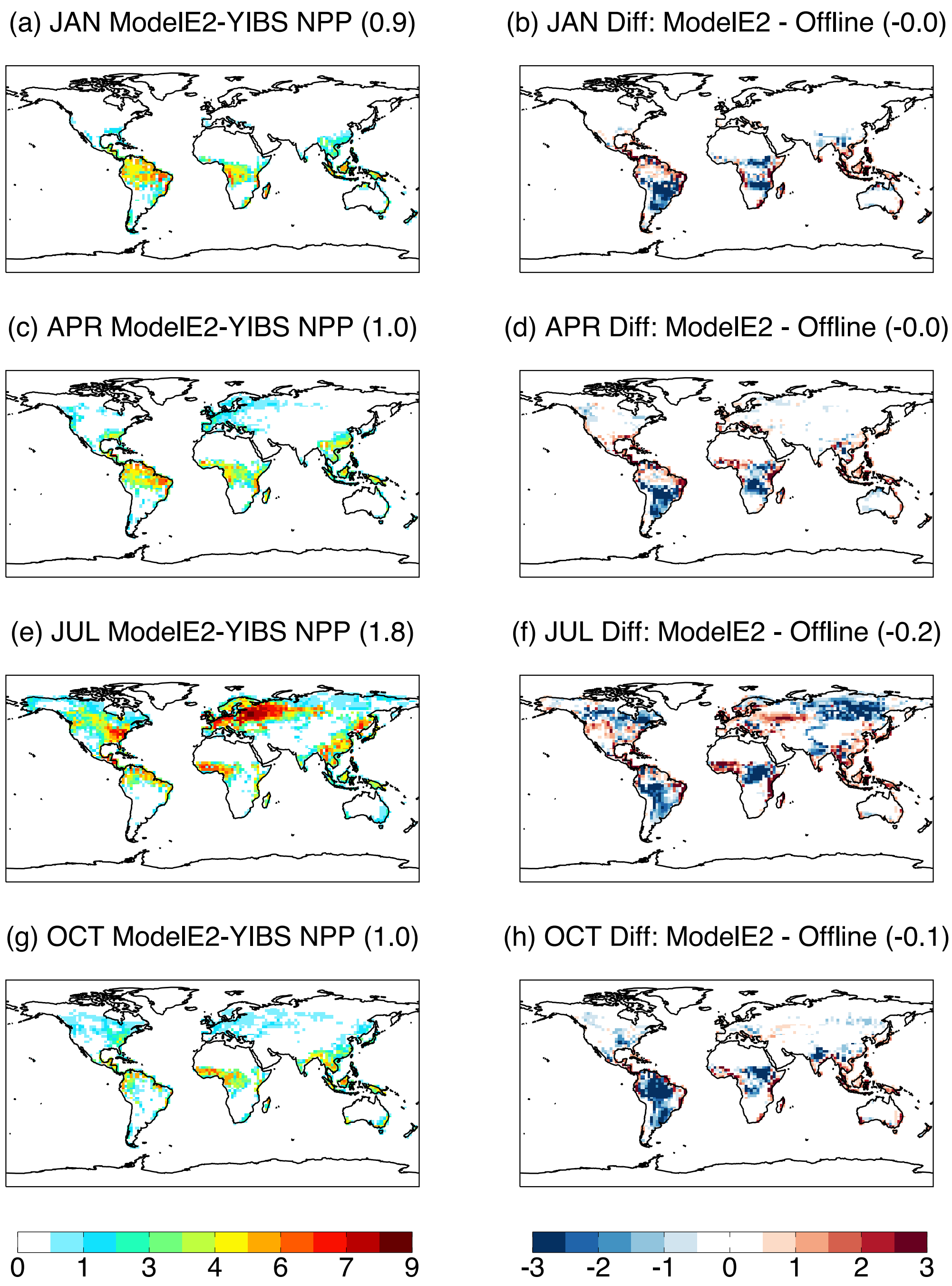

Figure S8. Simulated (left) net primary productivity (NPP) with ModelE2-YIBs and (right) its differences relative to simulations with offline YIBs driven by WFDEI reanalysis for period 1996-2005. Each row represents results averaged for a specific month. Units: g m^{-2} day^{-1}.

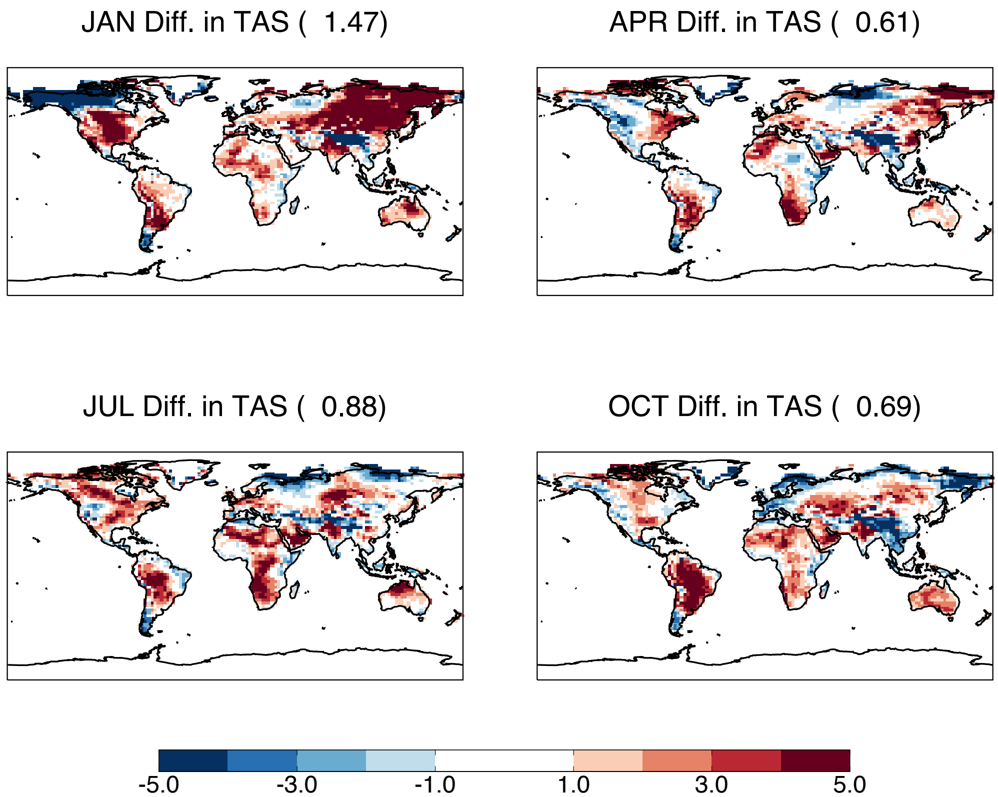

Figure S9. Differences of surface air temperature between ModelE2-YIBs and WFDEI for period 1996-2005. Each panel represents results averaged for a specific month. Units: °C.

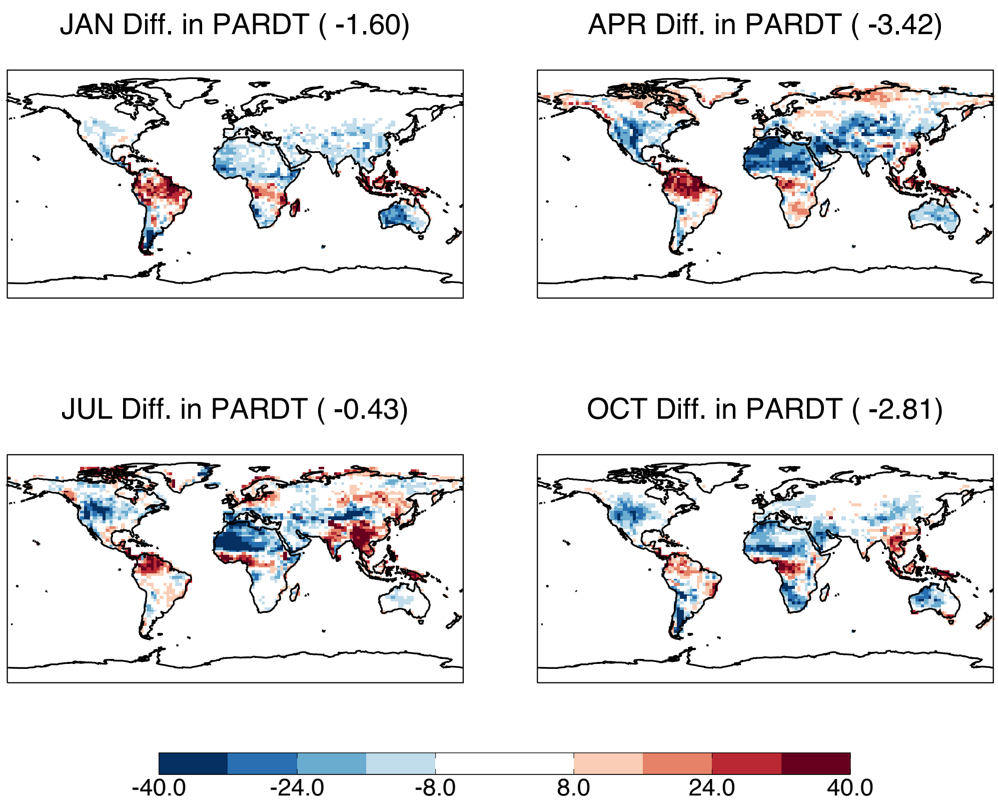

Figure S10. Differences of total Photosynthetically active radiation (PAR) between ModelE2-YIBs and WFDEI for period 1996-2005. Each panel represents results averaged for a specific month. Units: W m^{-2}.

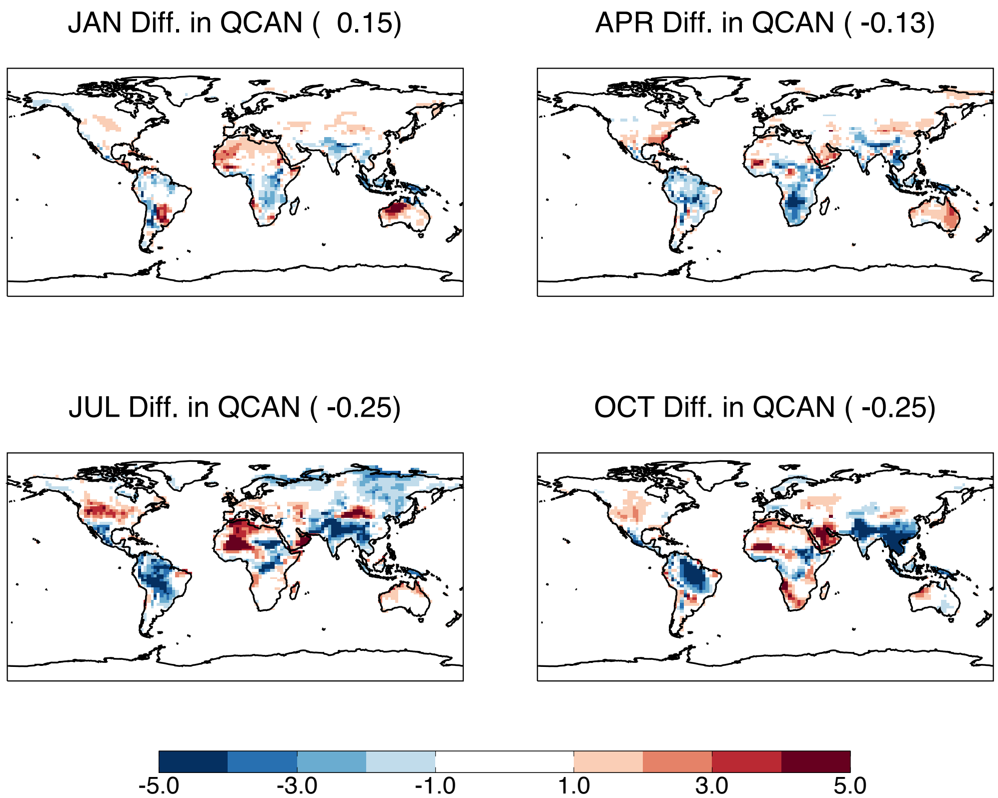

Figure S11. Differences of canopy humidity between ModelE2-YIBs and WFDEI for period 1996-2005. Each panel represents results averaged for a specific month. Units: g kg^{-1}.

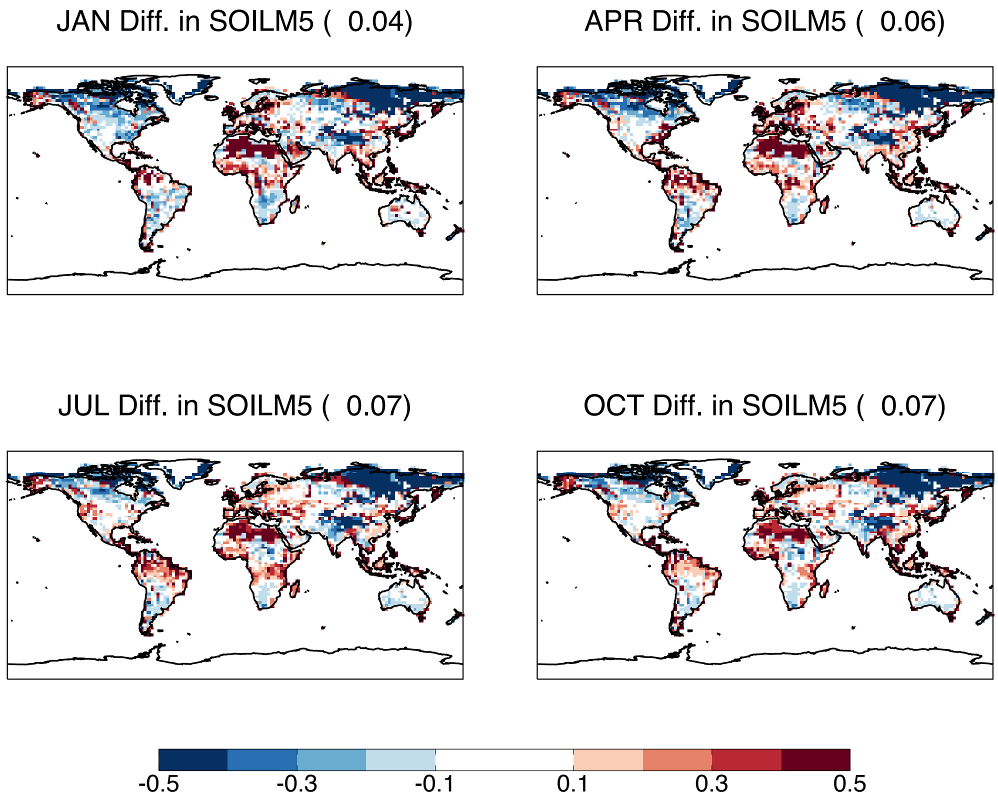

Figure S12. Differences of soil wetness at the 5th soil layer (~1.5 m) between ModelE2-YIBs and WFDEI for period 1996-2005. Each panel represents results averaged for a specific month. Units: fraction.

Table S1. Descriptions of 145 flux tower sites from NACP and FLUXNET [a].

Site	PFT	Start	End	Longitude	Latitude	Country	Source
AT-Neu	GRA	2002	2004	11.32°E	47.12°N	Austria	FLUXNET
AU-Fog	SHR	2006	2007	131.31°E	12.54°S	Australia	FLUXNET
AU-How	SHR	2001	2006	131.15°E	12.49°S	Australia	FLUXNET
AU-Tum	EBF	2001	2006	148.15°E	35.66°S	Australia	FLUXNET
AU-Wac	EBF	2005	2007	145.19°E	37.43°S	Australia	FLUXNET
BE-Bra	ENF	1997	2006	4.52°E	51.31°N	Belgium	FLUXNET
BE-Jal	ENF	2006	2006	6.07°E	50.56°N	Belgium	FLUXNET
BE-Lon	CRO	2004	2006	4.75°E	50.55°N	Belgium	FLUXNET
BE-Vie	ENF	1996	2006	6°E	50.31°N	Belgium	FLUXNET
BR-Sa3	EBF	2000	2003	54.97°W	3.02°S	Brazil	FLUXNET
BW-Ma1	SHR	1999	2001	23.56°E	19.92°S	Botswana	FLUXNET
CA-Ca1	ENF	1998	2006	125.33°W	49.87°N	Canada	NACP
CA-Ca2	ENF	2001	2006	125.29°W	49.87°N	Canada	NACP
CA-Ca3	ENF	2002	2006	124.9°W	49.54°N	Canada	NACP
CA-Gro	ENF	2004	2006	82.16°W	48.22°N	Canada	NACP
CA-Let	GRA	1997	2007	112.94°W	49.71°N	Canada	NACP
CA-Man	ENF	1994	2003	98.48°W	55.88°N	Canada	FLUXNET
CA-Mer	SHR	1999	2006	75.52°W	45.41°N	Canada	NACP
CA-NS1	ENF	2002	2005	98.48°W	55.88°N	Canada	FLUXNET
CA-NS2	ENF	2001	2005	98.53°W	55.91°N	Canada	FLUXNET
CA-NS3	ENF	2001	2005	98.38°W	55.91°N	Canada	FLUXNET
CA-NS4	ENF	2002	2004	98.38°W	55.91°N	Canada	FLUXNET
CA-NS5	ENF	2001	2005	98.49°W	55.86°N	Canada	FLUXNET
CA-NS6	SHR	2001	2005	98.96°W	55.92°N	Canada	FLUXNET
CA-NS7	SHR	2002	2005	99.95°W	56.64°N	Canada	FLUXNET
CA-Oas	DBF	1997	2006	106.2°W	53.63°N	Canada	NACP
CA-Obs	ENF	2000	2006	105.12°W	53.99°N	Canada	NACP
CA-Ojp	ENF	2000	2006	104.69°W	53.92°N	Canada	NACP
CA-Qcu	ENF	2001	2006	74.04°W	49.27°N	Canada	FLUXNET
CA-Qfo	ENF	2004	2006	74.34°W	49.69°N	Canada	NACP
CA-SJ1	ENF	2002	2005	104.66°W	53.91°N	Canada	NACP
CA-SJ2	ENF	2003	2006	104.65°W	53.95°N	Canada	NACP
CA-SJ3	ENF	2005	2006	104.65°W	53.88°N	Canada	NACP
CA-TP4	ENF	2002	2007	80.36°W	42.71°N	Canada	NACP
CA-WP1	SHR	2003	2007	112.47°W	54.95°N	Canada	NACP
CH-Oe1	GRA	2002	2006	7.73°E	47.29°N	Switzerland	FLUXNET
CH-Oe2	CRO	2005	2005	7.73°E	47.29°N	Switzerland	FLUXNET
CZ-BK1	ENF	2000	2006	18.54°E	49.5°N	Czech Republic	FLUXNET
DE-Bay	ENF	1996	1999	11.87°E	50.14°N	Germany	FLUXNET

Table S1. Continued.

Site	PFT	Start	End	Longitude	Latitude	Country	Source
DE-Geb	CRO	2004	2006	10.91°E	51.1°N	Germany	FLUXNET
DE-Gri	GRA	2005	2006	13.51°E	50.95°N	Germany	FLUXNET
DE-Hai	DBF	2000	2006	10.45°E	51.08°N	Germany	FLUXNET
DE-Kli	CRO	2004	2006	13.52°E	50.89°N	Germany	FLUXNET
DE-Meh	GRA	2003	2006	10.66°E	51.28°N	Germany	FLUXNET
DE-Tha	ENF	1996	2006	13.57°E	50.96°N	Germany	FLUXNET
DE-Wet	ENF	2002	2006	11.46°E	50.45°N	Germany	FLUXNET
DK-Lva	GRA	2005	2006	12.08°E	55.68°N	Denmark	FLUXNET
DK-Ris	CRO	2004	2005	12.1°E	55.53°N	Denmark	FLUXNET
DK-Sor	DBF	1996	2006	11.65°E	55.49°N	Denmark	FLUXNET
ES-ES1	ENF	1999	2006	0.32°W	39.35°N	Spain	FLUXNET
ES-ES2	CRO	2004	2006	0.32°W	39.28°N	Spain	FLUXNET
ES-LMa	SHR	2004	2006	5.77°W	39.94°N	Spain	FLUXNET
ES-VDA	GRA	2004	2006	1.45°E	42.15°N	Spain	FLUXNET
FI-Hyy	ENF	1996	2006	24.3°E	61.85°N	Finland	FLUXNET
FI-Kaa	SHR	2000	2006	27.3°E	69.14°N	Finland	FLUXNET
FI-Sod	ENF	2000	2006	26.64°E	67.36°N	Finland	FLUXNET
FR-Fon	DBF	2005	2006	2.78°E	48.48°N	France	FLUXNET
FR-Gri	CRO	2005	2006	1.95°E	48.84°N	France	FLUXNET
FR-Hes	DBF	1997	2006	7.07°E	48.67°N	France	FLUXNET
FR-LBr	ENF	1996	2006	0.77°W	44.72°N	France	FLUXNET
FR-Lq1	GRA	2004	2006	2.74°E	45.64°N	France	FLUXNET
FR-Lq2	GRA	2004	2006	2.74°E	45.64°N	France	FLUXNET
FR-Pue	EBF	2000	2006	3.6°E	43.74°N	France	FLUXNET
HU-Bug	GRA	2002	2006	19.6°E	46.69°N	Hungary	FLUXNET
HU-Mat	GRA	2004	2006	19.73°E	47.85°N	Hungary	FLUXNET
ID-Pag	EBF	2002	2003	114.04°E	2.35°N	Indonesia	FLUXNET
IE-Ca1	CRO	2004	2006	6.92°W	52.86°N	Ireland	FLUXNET
IE-Dri	GRA	2003	2005	8.75°W	51.99°N	Ireland	FLUXNET
IL-Yat	ENF	2001	2006	35.05°E	31.35°N	Israel	FLUXNET
IT-Amp	GRA	2002	2006	13.61°E	41.9°N	Italy	FLUXNET
IT-BCi	CRO	2004	2006	14.96°E	40.52°N	Italy	FLUXNET
IT-Col	DBF	1996	2006	13.59°E	41.85°N	Italy	FLUXNET
IT-Cpz	EBF	1997	2006	12.38°E	41.71°N	Italy	FLUXNET
IT-LMa	GRA	2003	2006	7.16°E	45.58°N	Italy	FLUXNET
IT-Lav	ENF	2000	2006	11.28°E	45.96°N	Italy	FLUXNET
IT-Lec	EBF	2005	2006	11.27°E	43.31°N	Italy	FLUXNET
IT-MBo	GRA	2003	2006	11.05°E	46.02°N	Italy	FLUXNET
IT-Mal	GRA	2003	2006	11.7°E	46.12°N	Italy	FLUXNET

Table S1. Continued.

Site	PFT	Start	End	Longitude	Latitude	Country	Source
IT-Non	DBF	2001	2006	11.09°E	44.69°N	Italy	FLUXNET
IT-PT1	DBF	2002	2004	9.06°E	45.2°N	Italy	FLUXNET
IT-Pia	SHR	2002	2005	10.08°E	42.58°N	Italy	FLUXNET
IT-Ren	ENF	1999	2006	11.44°E	46.59°N	Italy	FLUXNET
IT-Ro1	DBF	2000	2006	11.93°E	42.41°N	Italy	FLUXNET
IT-Ro2	DBF	2002	2006	11.92°E	42.39°N	Italy	FLUXNET
IT-SRo	ENF	1999	2006	10.28°E	43.73°N	Italy	FLUXNET
NL-Ca1	GRA	2003	2006	4.93°E	51.97°N	Netherlands	FLUXNET
NL-Hor	GRA	2004	2006	5.07°E	52.03°N	Netherlands	FLUXNET
NL-Lan	CRO	2005	2006	4.9°E	51.95°N	Netherlands	FLUXNET
NL-Loo	ENF	1996	2006	5.74°E	52.17°N	Netherlands	FLUXNET
PL-wet	SHR	2004	2005	16.31°E	52.76°N	Poland	FLUXNET
PT-Esp	EBF	2002	2006	8.6°W	38.64°N	Portugal	FLUXNET
PT-Mi1	EBF	2003	2005	8°W	38.54°N	Portugal	FLUXNET
PT-Mi2	GRA	2004	2006	8.03°W	38.48°N	Portugal	FLUXNET
RU-Fyo	ENF	1998	2004	32.92°E	56.46°N	Russia	FLUXNET
SE-Deg	SHR	2001	2005	19.55°E	64.18°N	Sweden	FLUXNET
SE-Faj	SHR	2005	2006	13.55°E	56.27°N	Sweden	FLUXNET
SE-Fla	ENF	1996	2002	19.46°E	64.11°N	Sweden	FLUXNET
SE-Nor	ENF	1996	2005	17.48°E	60.09°N	Sweden	FLUXNET
SE-Sk1	ENF	2005	2005	17.92°E	60.13°N	Sweden	FLUXNET
SE-Sk2	ENF	2004	2005	17.84°E	60.13°N	Sweden	FLUXNET
UK-AMo	SHR	2005	2005	3.24°W	55.79°N	UK	FLUXNET
UK-EBu	GRA	2004	2006	3.21°W	55.87°N	UK	FLUXNET
UK-ESa	CRO	2003	2005	2.86°W	55.91°N	UK	FLUXNET
UK-Gri	ENF	1997	2006	3.8°W	56.61°N	UK	FLUXNET
UK-Ham	DBF	2004	2005	0.86°W	51.15°N	UK	FLUXNET
UK-PL3	DBF	2005	2006	1.27°W	51.45°N	UK	FLUXNET
US-ARM	GRA	2000	2007	97.49°W	36.6°N	US	NACP
US-Aud	GRA	2002	2006	110.51°W	31.59°N	US	FLUXNET
US-Bar	DBF	2004	2005	71.29°W	44.07°N	US	FLUXNET
US-Bkg	GRA	2004	2006	96.84°W	44.35°N	US	FLUXNET
US-Blo	ENF	1997	2006	120.63°W	38.9°N	US	FLUXNET
US-Bo1	CRO	1996	2007	88.29°W	40.01°N	US	FLUXNET
US-Dk3	ENF	1998	2005	79.09°W	35.98°N	US	NACP
US-FPe	GRA	2000	2006	105.1°W	48.31°N	US	FLUXNET
US-Goo	GRA	2002	2006	89.87°W	34.26°N	US	FLUXNET
US-Ha1	DBF	1991	2006	72.17°W	42.54°N	US	NACP
US-Ho1	ENF	1996	2004	68.74°W	45.2°N	US	NACP

Table S1. Continued.

Site	PFT	Start	End	Longitude	Latitude	Country	Source
US-Ho2	ENF	1999	2004	68.75°W	45.21°N	US	FLUXNET
US-IB1	CRO	2005	2007	88.22°W	41.86°N	US	NACP
US-IB2	GRA	2004	2007	88.24°W	41.84°N	US	NACP
US-Los	SHR	2000	2006	89.98°W	46.08°N	US	NACP
US-MMS	DBF	1999	2006	86.41°W	39.32°N	US	NACP
US-MOz	DBF	2004	2007	92.2°W	38.74°N	US	NACP
US-Me2	ENF	2002	2007	121.56°W	44.45°N	US	NACP
US-Me3	ENF	2004	2005	121.61°W	44.32°N	US	NACP
US-Me4	ENF	1996	2000	121.62°W	44.5°N	US	FLUXNET
US-Me5	ENF	1999	2002	121.57°W	44.44°N	US	NACP
US-NR1	ENF	1998	2007	105.55°W	40.03°N	US	NACP
US-Ne1	CRO	2001	2006	96.48°W	41.17°N	US	NACP
US-Ne2	CRO	2001	2006	96.47°W	41.17°N	US	NACP
US-Ne3	CRO	2001	2006	96.44°W	41.18°N	US	NACP
US-Oho	DBF	2004	2005	83.84°W	41.56°N	US	FLUXNET
US-PFa	ENF	1995	2005	90.27°W	45.95°N	US	NACP
US-SO2	SHR	1998	2006	116.62°W	33.37°N	US	NACP
US-SP1	ENF	2000	2005	82.22°W	29.74°N	US	FLUXNET
US-SP2	ENF	1998	2004	82.25°W	29.77°N	US	FLUXNET
US-SP3	ENF	1999	2004	82.16°W	29.76°N	US	FLUXNET
US-Shd	GRA	1997	2000	96.68°W	36.93°N	US	NACP
US-Syv	ENF	2001	2006	89.35°W	46.24°N	US	NACP
US-Ton	SHR	2001	2007	120.97°W	38.43°N	US	NACP
US-UMB	DBF	1999	2006	84.71°W	45.56°N	US	NACP
US-Var	GRA	2000	2007	120.95°W	38.41°N	US	NACP
US-WBW	DBF	1995	1999	84.29°W	35.96°N	US	FLUXNET
US-WCr	DBF	1998	2006	90.08°W	45.81°N	US	NACP
ZA-Kru	SHR	2001	2003	31.5°E	25.02°S	South Africa	FLUXNET

[a] The NACP site information is adopted from Schaefer et al. (2012), except that the operational time span listed here is only for the period when measurements of GPP are available. Most of NACP sites are also part of the FLUXNET network.
[b] PFT names are: evergreen needleleaf forest (ENF), deciduous broadleaf forest (DBF), shrublands (SHR), grasslands (GRA), and croplands (CRO). Some site biome definitions are attributed to the closet model PFT. For example, closed shrublands, permanent wetlands, and woody savannas are attributed to shrublands. Mixed forests are attributed to ENF.

References

Batjes, N. H.: Harmonized soil profile data for applications at global and continental scales: updates to the WISE database, Soil Use Manage, 25, 124-127, doi:10.1111/J.1475-2743.2009.00202.X, 2009.

Clark, D. B., Mercado, L. M., Sitch, S., Jones, C. D., Gedney, N., Best, M. J., Pryor, M., Rooney, G. G., Essery, R. L. H., Blyth, E., Boucher, O., Harding, R. J., Huntingford, C., and Cox, P. M.: The Joint UK Land Environment Simulator (JULES), model description - Part 2: Carbon fluxes and vegetation dynamics, Geosci Model Dev, 4, 701-722, doi:10.5194/Gmd-4-701-2011, 2011.

Huntzinger, D. N., Schwalm, C., Michalak, A. M., Schaefer, K., King, A. W., Wei, Y., Jacobson, A., Liu, S., Cook, R. B., Post, W. M., Berthier, G., Hayes, D., Huang, M., Ito, A., Lei, H., Lu, C., Mao, J., Peng, C. H., Peng, S., Poulter, B., Riccuito, D., Shi, X., Tian, H., Wang, W., Zeng, N., Zhao, F., and Zhu, Q.: The North American Carbon Program Multi-Scale Synthesis and Terrestrial Model Intercomparison Project - Part 1: Overview and experimental design, Geosci Model Dev, 6, 2121-2133, doi:10.5194/Gmd-6-2121-2013, 2013.

Piao, S. L., Sitch, S., Ciais, P., Friedlingstein, P., Peylin, P., Wang, X. H., Ahlstrom, A., Anav, A., Canadell, J. G., Cong, N., Huntingford, C., Jung, M., Levis, S., Levy, P. E., Li, J. S., Lin, X., Lomas, M. R., Lu, M., Luo, Y. Q., Ma, Y. C., Myneni, R. B., Poulter, B., Sun, Z. Z., Wang, T., Viovy, N., Zaehle, S., and Zeng, N.: Evaluation of terrestrial carbon cycle models for their response to climate variability and to CO2 trends, Global Change Biol, 19, 2117-2132, doi:10.1111/Gcb.12187, 2013.

Sitch, S., Friedlingstein, P., Gruber, N., Jones, S. D., Murray-Tortarolo, G., Ahlström, A., Doney, S. C., Graven, H., Heinze, C., Huntingford, C., Levis, S., Levy, P. E., Lomas, M., Poulter, B., Viovy, N., Zaehle, S., Zeng, N., Arneth, A., Bonan, G., Bopp, L., Canadell, J. G., Chevallier, F., Ciais, P., Ellis, R., Gloor, M., Peylin, P., Piao, S. L., Quéré, C. L., Smith, B., Zhu, Z., and Myneni, R.: Recent trends and drivers of regional sources and sinks of carbon dioxide, Biogeosciences, 12, 653-679, 2015.

Wutzler, T. and Reichstein, M.: Soils apart from equilibrium - consequences for soil carbon balance modelling, Biogeosciences, 4, 125-136, 2007.